Identification of defined structural elements within TOR2 kinase required for TOR complex 2 assembly and function in *Saccharomyces cerevisiae*

Jennifer Tsverov, Kristina Yegorov, and Ted Powers*
Department of Molecular and Cellular Biology, College of Biological Sciences, University of California, Davis, Davis, CA 95616

ABSTRACT **The mammalian target of rapamycin (mTOR) is a large protein kinase that assembles into two multisubunit protein complexes, mTORC1 and mTORC2, to regulate cell growth in eukaryotic cells. While significant progress has been made in our understanding of the composition and structure of these complexes, important questions remain regarding the role of specific sequences within mTOR important for complex formation and activity. To address these issues, we have used a molecular genetic approach to explore TOR complex assembly in budding yeast, where two closely related TOR paralogues, TOR1 and TOR2, partition preferentially into TORC1 versus TORC2, respectively. We previously identified an ~500-amino-acid segment within the N-terminal half of each protein, termed the major assembly specificity (MAS) domain, which can govern specificity in formation of each complex. In this study, we have extended the use of chimeric TOR1-TOR2 genes as a "sensitized" genetic system to identify specific subdomains rendered essential for TORC2 function, using synthetic lethal interaction analyses. Our findings reveal important design principles underlying the dimeric assembly of TORC2 as well as identifying specific segments within the MAS domain critical for TORC2 function, to a level approaching single-amino-acid resolution. Together these findings highlight the complex and cooperative nature of TOR complex assembly and function.**

Monitoring Editor
Doug Kellogg
University of California, Santa Cruz

Received: Dec 10, 2021
Revised: Mar 1, 2022
Accepted: Mar 8, 2022

INTRODUCTION

The mammalian target of rapamycin (mTOR) network is a conserved regulator of eukaryotic cell growth and cellular homeostasis, contributes to aging, and is dysregulated in many human diseases, including cancer (Wullschleger *et al.*, 2006; Saxton and Sabatini, 2017; Mossmann *et al.*, 2018; Magaway *et al.*, 2019). The central component in this network is the large (~280 kDa) mTOR protein, a Ser/Thr protein kinase and member of the conserved PIKK-related family of protein kinases (Bosotti *et al.*, 2000; Wullschleger *et al.*, 2006). In addition to a conserved C-terminal kinase domain and adjacent FRB domain that interacts with rapamycin, mTOR is composed almost entirely of helical repeats, including N-terminal and middle HEAT (N-HEAT and M-HEAT, respectively) and FAT/TPR repeat domains (Andrade and Bork, 1995; Andrade *et al.*, 2001; Knutson, 2010; Tafur *et al.*, 2020). mTOR functions as part of two distinct protein complexes, mTORC1 and mTORC2, where mTORC1 is uniquely inhibited by the macrolide antibiotic rapamycin (Kim *et al.*, 2002; Loewith *et al.*, 2002; Jacinto *et al.*, 2004; Sarbassov *et al.*, 2004; Wullschleger *et al.*, 2006; Eltschinger and Loewith, 2016; Tafur *et al.*, 2020). In addition to mTOR, mTORC1 includes as core components Raptor and mLST8/GβL, while mTORC2 includes Rictor, SIN1, and mLST8/GβL (Hara *et al.*, 2002; Kim *et al.*, 2002, 2003; Sarbassov *et al.*, 2004; Eltschinger and Loewith, 2016). Association with complex-specific partners and regulators is proposed to control their intracellular localization as well as governing substrate selection and regulating mTOR kinase activity (Eltschinger and Loewith, 2016; Yang *et al.*, 2017).

This article was published online ahead of print in MBoC in Press (http://www.molbiolcell.org/cgi/doi/10.1091/mbc.E21-12-0611) on March 16, 2022.

*Address correspondence to: Ted Powers (tpowers@ucdavis.edu).

Abbreviations used: TOR, target of rapamycin; TORC1, TOR complex 1; TORC2, TOR complex 2.

Our understanding of the structure and function of mTORC1 and mTORC2 has advanced considerably in recent years, aided by parallel studies in budding yeast, *Saccharomyces cerevisiae*, where two TOR paralogues, TOR1 and TOR2, assemble with a conserved core set of orthologous proteins to form TORC1 and TORC2 (Loewith *et al.*, 2002; Wedaman *et al.*, 2003; Reinke *et al.*, 2004; Tafur *et al.*, 2020). Specifically, TORC1 contains either TOR1 or TOR2, as well as KOG1 (orthologue of Raptor), whereas TORC2 contains TOR2, AVO1 (orthologue of SIN1), and AVO3 (orthologue of Rictor). Both complexes contain LST8 (orthologue of mLST8/GβL) as a common subunit, as well as a number of nonconserved, complex-specific proteins, including AVO2 in TORC2 (Loewith *et al.*, 2002; Wedaman *et al.*, 2003; Reinke *et al.*, 2004; Tafur *et al.*, 2020). Models derived from biochemical and ultrastructural studies of both yeast and mammalian complexes indicate that they likely function as dimers and possess an overall rhomboid-like, symmetrical shape, determined primarily by the superhelical topology of the large N-terminal domain of TOR/mTOR (Wullschleger *et al.*, 2005; Yang *et al.*, 2013, 2016, 2017; Gaubitz *et al.*, 2015; Aylett *et al.*, 2016; BaretiL *et al.*, 2016; Karuppasamy *et al.*, 2017; Chen *et al.*, 2018; Stuttfeld *et al.*, 2018; Scaiola *et al.*, 2020). High-resolution (~3.0 Å) Cryogenic electron microscopy (Cryo-EM) models have emerged recently for both mTORC1 and mTORC2 (Yang *et al.*, 2017; Scaiola *et al.*, 2020), revealing key architectural details as well as insights into their regulation, for example evidence for conformation changes within the mTORC1 active site following interaction with the upstream activator Rheb (Yang *et al.*, 2017). Despite these advances, many important structural features within these models remain unresolved, particularly for mTORC2 (Scaiola *et al.*, 2020). Moreover, the role of specific amino acids within TOR/mTOR for complex assembly and function remains almost completely unknown. Finally, while structural models provide important information about macromolecular organization, to be useful they must be paired with other methods to examine structure–function relationships involved in complex assembly and activity, as well as test predictions regarding the significance of observed protein–protein contacts.

To address these gaps and to complement ongoing structural studies, we have employed a molecular genetic approach to interrogate the importance of specific elements within TOR1 and TOR2, taking advantage of their unique behavior in yeast, where TOR1 assembles exclusively into TORC1 and TOR2 assembles preferentially into TORC2 (Loewith *et al.*, 2002; Wedaman *et al.*, 2003; Reinke *et al.*, 2004). By constructing a set of TOR1-TOR2 chimeras, we previously identified an ~500-amino-acid domain corresponding to the N-HEAT domain, termed the major assembly specificity (MAS) domain, that can direct assembly of both TOR proteins into TORC1 versus TORC2 (Hill *et al.*, 2018) (Figure 1A). In our present study, we have extended this approach to probe the importance of predicted quaternary interactions involving specific TORC2 partners as well as exploring the role of specific features within the TOR2 MAS domain for TORC2 function. Our findings reveal unanticipated complexity for TORC2 assembly as well as identifying specific subdomains within the TOR2 MAS critical for TORC2 activity.

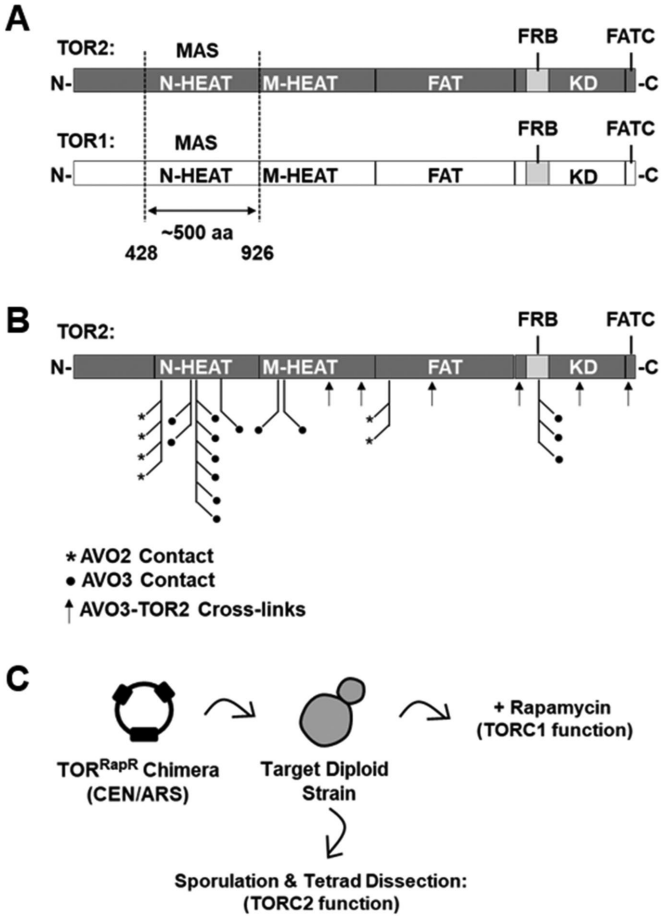

FIGURE 1: Overview and experimental approach. (A) Schematics showing the domain architecture of TOR1 and TOR2. The major assembly specificity (MAS) domain, which corresponds to the N-HEAT region of both TOR1 and TOR2 (Hill *et al.*, 2018), is depicted. (B) Predicted amino acid contacts between TOR2 and TORC2 components AVO2 (asterisks) and AVO3 (filled circles) within a model of TORC2 determined by Cryo-EM (Karuppasamy *et al.*, 2017). Contacts were identified using the structure analysis software tool UCSF Chimera (Pettersen *et al.*, 2004). Identified protein cross-links (Gaubitz *et al.*, 2015) between TOR2 and AVO3 (arrows) are also indicated. (C) Schematic of genetic approach to test chimeric TOR1-TOR2 genes for TORC1 and TORC2 function. See the text for details.

RESULTS

Strategy and experimental approach

Our prior study revealed that distinct regions of TOR2, in addition to the MAS/N-HEAT domain (for simplicity referred to here as TOR2 MAS), are sufficient but not necessary to confer TORC2 function (Hill *et al.*, 2018). These findings suggest that significant sequence flexibility exists within TOR2 to govern TORC2 assembly. In this context, we observed that many predicted sites of interaction between TOR2 and its TORC2-specific partners AVO2 and AVO3, based on a medium-resolution Cryo-EM structural model and protein–protein cross-linking data, map to discontinuous segments of TOR2 within several TOR1-TOR2 chimeras (Gaubitz *et al.*, 2015; Karuppasamy *et al.*, 2017; Hill *et al.*, 2018) (Figure 1B). We therefore sought to use these chimeras to interrogate the importance of predicted quaternary interactions for TORC2 assembly and function, using a synthetic sick/lethal (SSL) genetic interaction approach (Kaiser and Schekman, 1990; Guarente, 1993). This approach takes advantage of the fact that two mutations in interacting gene products, including within multiprotein complexes, often yield exacerbated phenotypes compared with either single mutation alone. Moreover, using genetic approaches, including synthetical lethality, to explore the function of paralogous gene products can yield information about both the architecture and the evolution of protein complexes (Mirny and Gelfand, 2002; Varga *et al.*, 2021). Our general strategy, adapted from our prior study

(Hill *et al.*, 2018), was to introduce chimeric TOR genes into target heterozygous diploid strains, followed by sporulation, tetrad dissection, and phenotypic analysis to assess TOR2 and, by extension, TORC2 function (Figure 1C). Unless stated otherwise, each chimera also harbored the dominant rapamycin resistance (RapR) allele (Heitman *et al.*, 1991) to allow for qualitative assessment of TORC1 activity (Figure 1C).

Evidence for essential quaternary interactions within TORC2

On the basis of our prior findings (Hill *et al.*, 2018), we reconstructed representative chimeras that span the range of predicted TOR2 interactions with AVO2 and AVO3 (Figures 1B and 2A). Because the essential TORC2-specific subunit AVO1 (orthologue of mammalian SIN1) is predicted to interact exclusively with the C-terminal region of TOR2 (Gaubitz *et al.*, 2015; Karuppasamy *et al.*, 2017), we did not address its role in TORC2 assembly in this study. Chimeras were constructed using synthetic gene synthesis and seamless gene cloning methods, where each construct contained three copies of the HA epitope at the N-terminus (see *Materials and Methods*). Western blot analysis demonstrated that each chimera produced normal levels of TOR protein (Figure 2D).

We first tested the ability of these chimeras to replace endogenous TOR2 within TORC2 in the absence of the nonessential TORC2 component AVO2. Plasmids expressing these chimeras were introduced into a double heterozygous TOR2/tor2Δ AVO2/avo2Δ strain, followed by sporulation and tetrad dissection. For comparison, we also tested a plasmid that expressed full-length TOR2 (pPL632). As expected and consistent with our previous findings (Hill *et al.*, 2018), cells singly deleted for either tor2Δ or avo2Δ were viable in the presence of each of these chimeras. We next scored the frequency of isolating haploid strains that harbored both tor2Δ and avo2Δ mutations and a chimera plasmid (described as percent viability) as well as scoring relative colony sizes of resulting viable haploid strains. We observed that full-length TOR2 and a chimera containing the entire N-terminus of TOR2 (pPL630) (Helliwell *et al.*, 1994; Hill *et al.*, 2018) were each viable in tor2Δ avo2Δ cells (Figure 2B). By contrast, chimeras containing either the TOR2 MAS domain (pPL626) or the reciprocal chimera containing the TOR1 MAS domain (pPL655) failed to support the growth of tor2Δ avo2Δ cells (Figure 2B). We conclude from these results that TOR2-specific sequences throughout the N-terminal region of TOR2 are required for proper TORC2 function in the absence of AVO2.

To extend these results, we next tested the ability of these chimeras to provide TOR2 function in a strain that harbored a truncated allele of AVO3 lacking 147 amino acids at its C-terminus (termed avo3-ΔCT). Previous studies demonstrated that this allele is functional yet causes TORC2 to become sensitive to rapamycin, where it is proposed to increase access of the FRBP-rapamycin complex to the FRB domain (Gaubitz *et al.*, 2015). Given that AVO3 is encoded by an essential gene and, therefore, we could not analyze a null allele, we used avo3-ΔCT as a possible hypomorphic mutant. As expected, full-length TOR2 (pPL632) supported viability in tor2Δ avo3-ΔCT cells (Figure 2C). By contrast, as was observed in avo2Δ cells, both the TOR2 MAS domain (pPL626) and TOR1 MAS domain (pPL655) chimeras displayed synthetic lethal interactions with the avo3-ΔCT allele (Figure 2C). Interestingly, we observed that the chimera containing the entire N-terminus of TOR2 (pPL630) conferred a severe synthetic phenotype in combination with the avo3-ΔCT allele (Figure 2C). We conclude from these results that TOR2-specific determinants throughout the length of the protein, including the FRB and kinase domains, are required for proper TORC2 function in cells harboring this truncated allele of AVO3.

A recent structural model for yeast TORC2, based on Cryo-EM analysis, includes only limited assigned densities corresponding to AVO2 and AVO3 (Karuppasamy *et al.*, 2017). Despite these limitations, we observed important correlations between chimera-specific phenotypes, described above, and the proximity of TOR2-specific sequences to both proteins. For AVO2, the TOR1 MAS (pPL655) and TOR2 MAS (pPL626) are each missing TOR2-unique sequences adjacent to AVO2, whereas these sequences are present in the complete N-terminal TOR2 chimera (pPL630) (Figure 2E). We note that each copy of AVO2 interacts with TOR2-specific sequences within a single TOR2 chain, suggesting that loss of AVO2 disrupts the assembly of individual TORC2 monomers (Figure 2E).

By contrast, only full-length TOR2 is functional in combination with the avo3-ΔCT allele, consistent with the fact that AVO3 makes extensive contacts throughout TOR2. Intriguingly, contacts with AVO3 are partitioned with respect to elements in a single TOR2 protein. Thus, the N-terminal MAS domain is predicted to interact with one AVO3 monomer, whereas the C-terminus, including the FRB domain, is in proximity to a second AVO3 monomer (Figure 2F, left panel). On the basis of our phenotypic analyses, we suggest that assembly and/or stability of TORC2 is likely to require interactions between TORC2 monomers that are anchored, in part, by interactions involving AVO3. Significantly, this arrangement of interactions is conserved in mTORC2, where in a recent high-resolution structural model (Scaiola *et al.*, 2020), the mTOR MAS domain contacts one Rictor monomer and the FRB domain interacts with a second copy of Rictor (Figure 2F, right panel).

The molecular basis for the observed synthetic interactions between TOR1-TOR2 chimeras and the avo3-ΔCT allele is unknown, as amino acids corresponding to this deletion are not resolved in the published model for TORC2 (Gaubitz *et al.*, 2015; Karuppasamy *et al.*, 2017). However, one possibility is that loss of C-terminal sequences in AVO3 disrupts interactions between monomers that make TORC2 activity dependent on the presence of TOR2-specific sequences adjacent to the FRB and/or kinase domain(s).

In the above experiments, except for the TOR1 MAS domain chimera (pPL655), all constructs contained the RapR allele and, as expected, conferred robust rapamycin resistance as well as rescuing the lethality of a tor2Δ strain (Figure 3). By contrast, when the RapR allele was introduced into the TOR1 MAS domain chimera (pPL655), the resulting construct (pPL651) conferred strong rapamycin resistance yet provided only weak rescue of the lethality of a tor2Δ strain (Figure 3). Western blot analysis demonstrated that chimeras 651 and 655 produced equivalent levels of protein, suggesting that deficiencies in steady state levels of TOR do not explain these phenotypic differences (Figure 3). While we do not understand the molecular basis for this apparent synthetic genetic interaction, it is consistent with our conclusion, described above, that functional interactions between the MAS and FRB domains are required for proper TORC2 function.

A sensitized genetic system to identify TOR2 elements essential for TORC2 function

Our above findings revealed novel genetic interactions between distinct TOR1-TOR2 chimeras and TORC2-specific partners. We reasoned that we could employ a similar approach to identify synthetic interactions within TOR2 (i.e., intragenic interactions), as an approach to refine our understanding of structural elements within TOR2 important for TORC2 function. We focused on the TOR2 MAS domain, where we showed previously that approximately 500 amino acids of TOR2 are sufficient to confer TORC2 function within the context of an otherwise full-length TOR1 protein (Hill *et al.*, 2018).

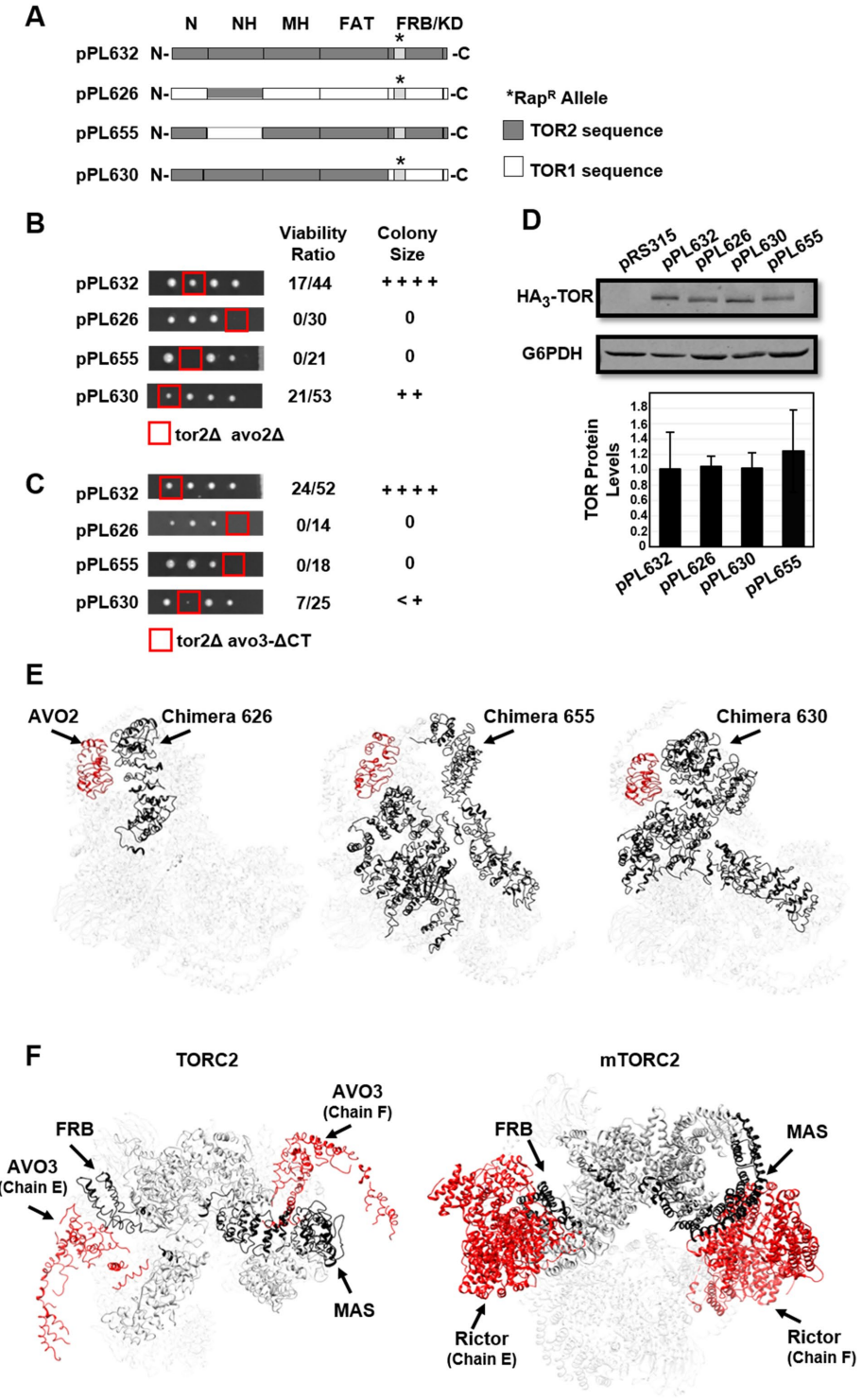

FIGURE 2: Synthetic genetic interactions involving TORC2 components. (A) Chimeric TOR1-TOR2 genes constructed for this study. Plasmid pPL632 expresses full-length TOR2. Plasmid pPL626 expresses the TOR2 MAS domain within the context of TOR1. The reciprocal chimera, pPL655, expresses the TOR1 MAS domain within the context of TOR2. Plasmid pPL630 expresses the complete N-terminal region of TOR2, including the FAT domain, but contains the TOR1 FRB and kinase domains. Where indicated, constructs harbor the rapamycin resistance mutation (RapR); this mutation corresponds to the TOR1-1 allele (S1972R) for sequences corresponding to TOR1 and the TOR2-1 allele (S1975R) for sequences corresponding to TOR2. (B) Chimeras described in A were introduced into a double heterozygous TOR2/tor2Δ AVO2/avo2Δ strain, followed by sporulation and tetrad dissection. Viable haploid progeny were genotyped by growth on selective media (see *Materials and Methods*). Viability was determined based on the number of tor2Δ avo2Δ haploid progeny that carried a plasmid compared with total tor2Δ progeny that carried a plasmid. The relative colony size was assessed following incubation at 30°C for 2 d on YPD solid media. ++++ corresponds to wild-type growth, and 0 corresponds to no growth. (C) Chimeras described in A were introduced into a double heterozygous TOR2/tor2Δ AVO3/avo3-Δ CT strain, followed by sporulation and tetrad dissection. Viable haploid progeny were genotyped by growth on selective media (see *Materials and Methods*). Viability was determined based on the number of tor2Δ avo3-Δ CT haploid progeny that carried a plasmid compared with total tor2Δ progeny that carried a plasmid. The relative colony size was assessed as in B. (D) Western blot analysis of TOR1-TOR2 chimeras. The indicated plasmids were introduced into a TOR2/tor2Δ heterozygous diploid strain (lanes 2–5). Cells were grown to mid–log phase in selective media, and protein extracts were prepared and analyzed by SDS–PAGE and immunoblotting. Blots were probed with anti-HA to detect plasmid-expressed TOR chimeras or anti-G6PDH (Zwf1) as a loading control. Plasmid pRS315 is an empty control vector. TOR protein levels were quantified following normalization to the G6PDH signal and represent averages of three independent experiments (± SD). (E) Modeling TOR2-specific regions in the TOR2 MAS domain (pPL626) (left panel) or TOR1 MAS domain (pPL655) (right panel) chimeras, respectively. TOR2-specific regions are highlighted in gray in the schematic diagrams and are shown in black in the Cryo-EM model for TORC2 (Karuppasamy *et al.*, 2017). AVO2 is shown in red. Protein chains are labeled according to nomenclature described in Karuppasamy *et al.* (2017). (F) Left panel: TOR2 MAS and FRB domains within TOR2 (chain A) are shown in black and both copies of AVO3 are shown in red within the Cryo-EM model for TORC2 (Karuppasamy *et al.*, 2017). Proximities between the FRB domain and one copy of AVO3 (chain E) and between the MAS domain and the second copy of AVO3 (chain F) are apparent. Protein chains are labeled according to nomenclature described in Karuppasamy *et al.* (2017). Right panel: mTOR MAS and FRB domains within mTOR (chain A) are shown in black and both copies of Rictor are shown in red within the Cryo-EM model for mTORC2 (Scaiola *et al.*, 2020). Proximities between the FRB domain and one copy of Rictor (chain E) and between the MAS domain and the second copy of Rictor (chain F) are apparent. Protein chains are labeled according to nomenclature described in Scaiola *et al.* (2020).

We constructed several new chimeras using the TOR2 MAS domain construct (pPL626) as a starting platform (see *Materials and*

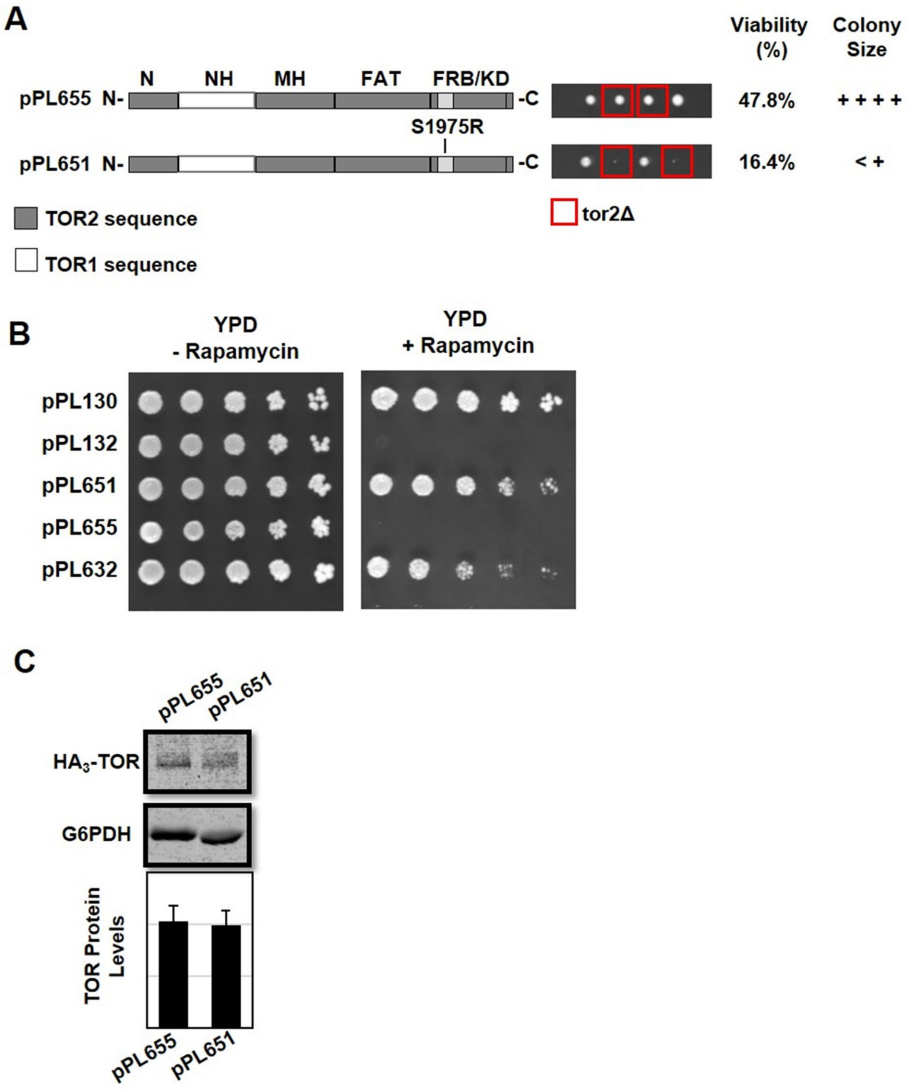

FIGURE 3: Introducing the TOR2-1 allele into the TOR1 MAS domain chimera is deleterious to TORC2 but not TORC1 function. (A) The TOR1 MAS domain chimera (pPL655) and the TOR1 MAS domain chimera containing the S1975R (RapR) TOR2-1 allele (pPL651) were introduced into heterozygous TOR2/tor2Δ cells and analyzed by tetrad dissection. Viability was determined based on the number of viable tor2Δ haploid progeny that carried a plasmid compared with all viable haploid progeny that carried a plasmid. The relative colony size was assessed following incubation at 30°C for 2 d on YPD solid media. (B) TOR2/tor2Δ cells carrying the indicated plasmids were tested for rapamycin resistance. Cells were grown in selective media to mid–log phase, serially diluted, and plated onto solid agar plates containing SCD minus leucine or SCD minus leucine and 0.2 μg/ml rapamycin. Plates were incubated at 30°C for 2 d and then photographed. As controls, plasmid pPL130 expresses the rapamycin resistance TOR1-1 allele and plasmid pPL132 expresses wild-type TOR1. (C) Western blot analysis of TOR1-TOR2 chimeras. TOR2/tor2Δ cells carrying the indicated plasmids were grown in selective media to mid–log phase, and protein extracts were prepared and analyzed as described in the legend to Figure 2D.

Methods). TOR2 activity was assessed by transformation of a TOR2/tor2Δ diploid strain, followed by sporulation and tetrad dissection. Here we scored both the frequency of finding haploid strains that harbored both a tor2Δ deletion and a chimera plasmid (described as percent viability) and their relative colony size. In parallel, we assessed the rapamycin resistance of each strain as a measure of TORC1 function as well as monitoring steady state levels of TOR protein by Western blot analysis.

In a first approach, we constructed "Minimal" (pPL628) and "Sub-Minimal" (pPL629) TOR2 MAS domain chimeras (Figure 4A). The TOR1/2 boundaries of these chimeras encompassed a central core of predicted TOR2 contacts for AVO2 and AVO3 (pPL628) or, alternatively, for AVO3 alone (pPL629) (Figure 1B) (Gaubitz *et al.*, 2015; Hill *et al.*, 2018). Surprisingly, the Minimal TOR2 MAS domain (pPL628) afforded only very limited TOR2 function, and the Sub-Minimal TOR2 MAS domain (pPL629) was completely nonfunctional as TOR2 (Figure 4A). Both chimeras produced normal levels of protein and conferred rapamycin resistance, consistent with an observed defect in TORC2 activity alone (Figure 4, B and C). To test whether the impaired phenotype of the Minimal TOR2 MAS domain was due to loss of TOR2-specific sequences at either end of this domain, we constructed two additional chimeras that restored TOR2 sequences at either the N-terminal side (Minimal MAS+N; pPL635) or the C-terminal side (Minimal MAS+C; pPL636), respectively. Each construct displayed only minor improvement in TOR2 phenotypes (Figure 4A). We conclude from this analysis that sequences outside the central core of the TOR2 MAS domain are required for proper TORC2 function. Surprisingly, we observed that Minimal MAS+C (pPL636) chimera also resulted in reduced rapamycin resistance and a significant reduction in the steady state level of TOR protein (Figure 4, B and C).

In a second approach, we tested whether the TOR2 MAS domain would tolerate the introduction of short stretches of TOR1 sequence interspersed throughout its length and retain TOR2 function. Accordingly, we constructed 10 chimeras (TOR2 MAS-A through TOR2 MAS-J), each representing a contiguous series of ~50-amino-acid segments of TOR1-specific sequences that replaced corresponding TOR2 sequences (Figure 5A) (see *Materials and Methods*). To maximize the likelihood of proper protein folding, chimeras were designed to maximize two criteria where possible: 1) TOR1-TOR2 boundaries ("switch points") were placed where TOR1 and TOR2 sequences were identical; and 2) each construct encompassed complete predicted α-helical repeat units (Perry and Kleckner, 2003; Knutson, 2010; Karuppasamy *et al.*, 2017). Chimeras were introduced into a TOR2/tor2Δ strain and analyzed as above. Here we observed surprising phenotypic diversity with respect to the level of rescue of tor2Δ lethality (Figure 5A). The most deleterious phenotypes were observed for chimeras that swapped sequences within the central region (chimeras E and F) of the MAS domain as well as at the N- and C-termini (chimeras A, B, and J) (Figure 5A). In particular, chimeras MAS-B and MAS-E were most impaired in their ability

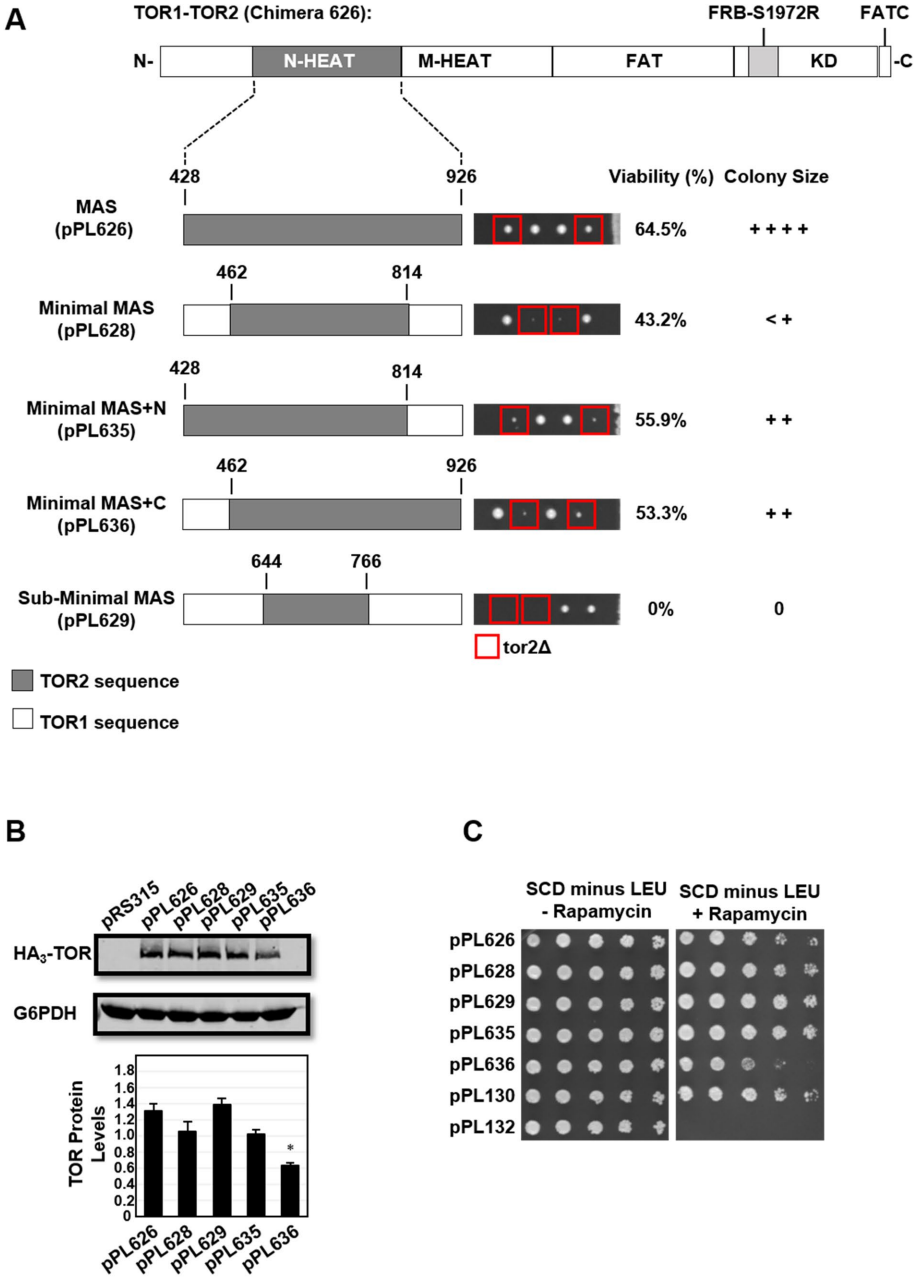

FIGURE 4: Testing the functionality of the central core of the TOR2 MAS domain. (A) TOR2 MAS domain plasmid pPL626 containing the S1972R (RapR) TOR1-1 allele was modified to create the indicated TOR1-TOR2 chimeras. Amino acid numbering refers to TOR2 protein sequence. "N" and "C" refer to N- and C-termini, respectively. Plasmids were introduced into heterozygous TOR2/tor2Δ cells and analyzed by tetrad analysis as described in the legend to Figure 3A. (B) Western blot analysis of TOR1-TOR2 chimeras. TOR2/tor2Δ cells carrying the indicated plasmids were grown in selective media to mid–log phase, and protein extracts were prepared and analyzed by SDS–PAGE and immunoblotting, as described in the legend to Figure 2D. (C) TOR2/tor2Δ cells carrying the indicated plasmids were tested for rapamycin resistance as described in the legend to Figure 3B.

to rescue the lethality of a tor2Δ strain (Figure 5A). Together these results both confirm that outer sequences of the TOR2 MAS domain are important for TORC2 function and highlight the importance of the central core of this domain.

All chimeras tested in this second approach produced full-length TOR protein and conferred resistance to rapamycin, an indication that they all assemble and function within TORC1 (Figure 5, B and C). However, three chimeras, MAS-A (pPL637), MAS-E (pPL641), and MAS-F (pPL642), resulted in significantly reduced steady state levels of protein and conferred weaker rapamycin resistance (Figure 5, B and C). We note that chimeras MAS-A (pPL637) and Minimal MAS+C (pPL636) share overlapping TOR1-specific sequences at the N-terminus of the TOR2 MAS domain, highlighting the sensitivity of this region to changes in TOR2-specific sequences (compare Figures 4 and 5). In addition, our findings that chimeras MAS-E and MAS-F result in reduced levels of TOR protein and impaired rapamycin resistance indicate that the central core of the TOR2 MAS domain is also sensitive to the precise composition of TOR1 versus TOR2 sequences and impact TOR complex assembly and/or TOR protein stability.

Fine dissection of TOR2 elements crucial for TORC2 function

To begin to understand, at the single-amino-acid level, the importance of elements within the TOR2 MAS domain, we focused on chimera TOR2 MAS-B, as introduction of TOR1-specific sequences into this relatively discrete region severely disrupted TORC2 function without affecting overall protein levels or TORC1 activity. We subdivided TOR2 MAS-B into three separate chimeras, MAS-B1 through MAS-B3, each representing approximately 6–10 amino acids of the TOR1 sequence within the context of an otherwise complete TOR2 MAS domain (Figure 6A). Each construct was introduced into a TOR2/tor2Δ strain and analyzed as above.

We observed that chimera MAS-B1 (pPL652) was severely impaired in its ability to rescue the lethality of a tor2Δ strain (Figure 6A). By contrast, chimeras MAS-B2 (pPL653) and MAS-B3 (pPL654) both provided near-wild-type rescue (Figure 6A). All three constructs produced normal levels of TOR protein and conferred strong rapamycin resistance (Figure 6, B and C). Remarkably, chimera MAS-B1 contains only 10 amino acids that differ between TOR1 and TOR2, with respect to the 498 amino acids that constitute the TOR2 MAS domain, affirming the utility of this approach to reveal amino acids crucial for TORC2 function (Figure 6A). We observed that chimera MAS-B2 includes two predicted amino acid contacts for AVO2 within MAS-B (Figure 6A). However, these amino acids are identical in TOR1 and TOR2; thus, it is unlikely that they contribute directly to complex specificity, a conclusion consistent with our findings that this chimera supports full TOR2 activity.

We used a similar approach to dissect chimera MAS-E, which is significantly impaired in TORC2 activity but showed defects in

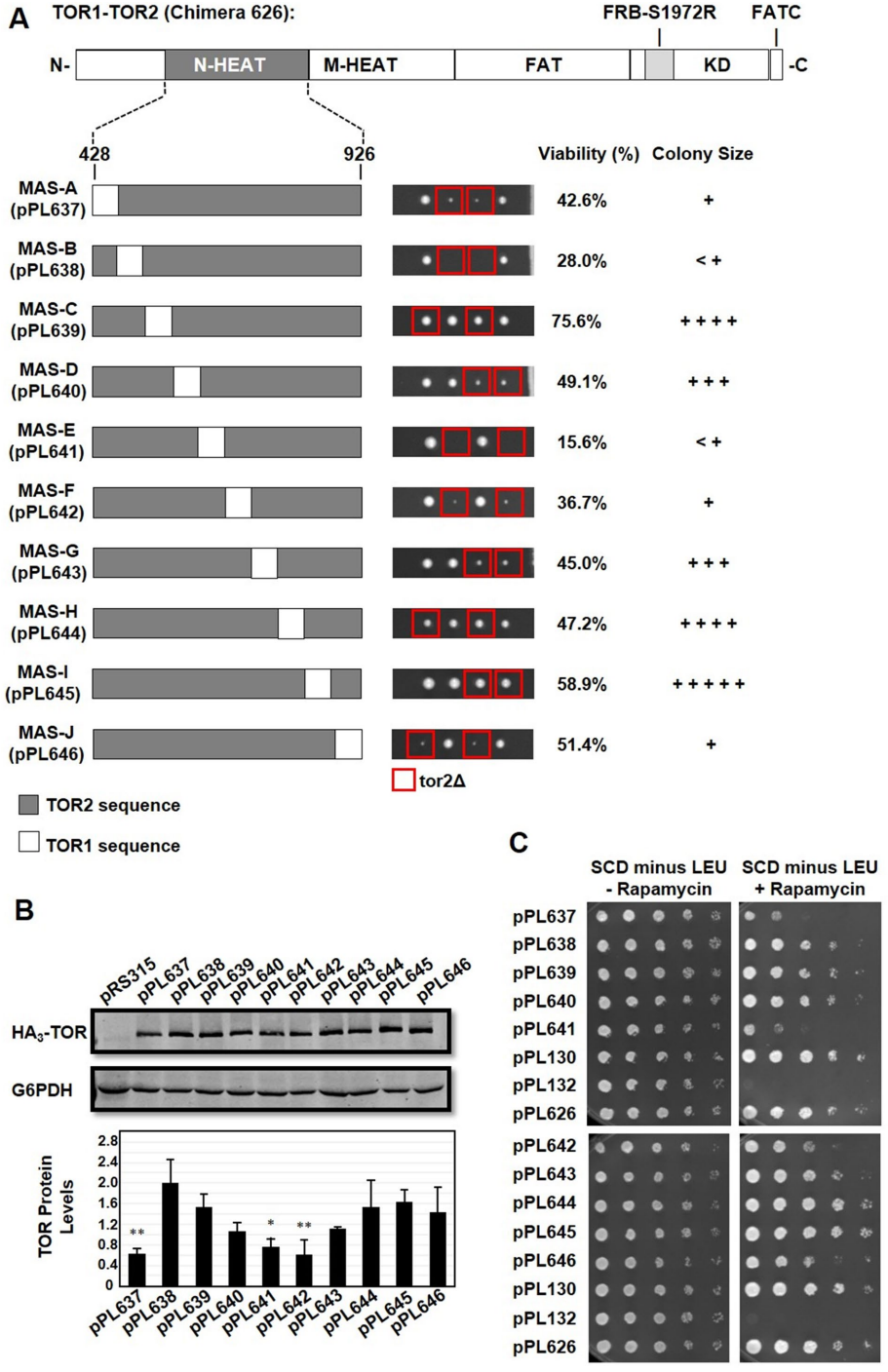

FIGURE 5: Systematic functional dissection of the TOR2 MAS domain. (A) TOR2 MAS domain plasmid pPL626containing the S1972R (RapR) TOR1-1 allele was modified to create the indicated TOR1-TOR2 chimeras. Each construct, MAS-A through MAS-J, contains approximately 50 amino acids of TOR1 sequence dispersed along the length of the TOR2 MAS domain. Plasmids were introduced into heterozygous TOR2/tor2Δ cells and analyzed by tetrad analysis as described in the legend to Figure 3A. (B) Western blot analysis of TOR1-TOR2 chimeras. TOR2/tor2Δ cells carrying the indicated plasmids were prepared and analyzed as described in the legend to Figure 2D. (C) TOR2/tor2Δ cells carrying the indicated plasmids were tested for rapamycin resistance as described in the legend to Figure 3B.

TORC1 as well (Figure 5). We subdivided chimera MAS-E into four separate constructs, MAS-E1 through MAS-E4, where each chimera possessed only four- to six-amino-acid differences between TOR1 and TOR2 with respect to the TOR2 MAS domain (Figure 7A). Interestingly, in contrast to the complete MAS-E chimera, all four constructs rescued a tor2Δ allele, produced normal levels of TOR protein, and provided strong rapamycin resistance (Figure 7, A–C). We note that two constructs, MAS-E3 (pPL649) and MAS-E4 (pPL650), displayed modest growth defects in tor2Δ cells, where MAS-E3 is the location of predicted sites of interaction between TOR2 and AVO3 (Figure 7A). We conclude from these findings that the TOR2 MAS domain can tolerate smaller clusters of TOR1 sequences within its central core and maintain adequate TORC2 activity, produce stable TOR protein, and function within TORC1.

DISCUSSION

In this study, we have used chimeric TOR1-TOR2 proteins to extend our understanding of specific determinants within TOR2 that are critical for TORC2 assembly and function. For example, the pattern of synthetic genetic interactions between TOR chimeras and mutant alleles of TORC2-specific components AVO2 and AVO3, examined within the context of a structural model for TORC2, suggests important design features for assembly of TORC2. In particular, our observation that proper TORC2 activity requires interactions between TOR2-specific elements within the context of the same TOR2 chain and both copies of AVO3 suggests that stable assembly of TORC2 requires complex quaternary interactions across the dimer interface. Because this arrangement of physical interactions is conserved between mTOR and Rictor, we predict that interactions between monomers will also turn out to be crucial for mTORC2 assembly and/or stability. Interestingly, an inspection of the structure of mTORC1 reveals that Raptor also makes contacts with both copies of mTOR within the mTORC1 dimer (Yang *et al.*, 2017), raising the interesting possibility that both mTORC1 and mTORC2 assemble as obligate dimers.

We previously identified the TOR2 MAS domain as a contiguous ~500-amino-acid segment within the N-terminus of TOR2 that is sufficient to confer TORC2 activity in the context of a TOR1-TOR2 chimera. We were surprised that we were unable to narrow this domain further, even though most predicted interactions between TOR2 and both AVO2 and AVO3 are located within a central ~200-amino-acid core of this domain. Instead, we systematically exchanged discrete segments within the TOR2 MAS domain, by introducing a "moving window" of TOR1 sequence, to identify specific clusters of essential TOR2-specific sequences. This approach employed a

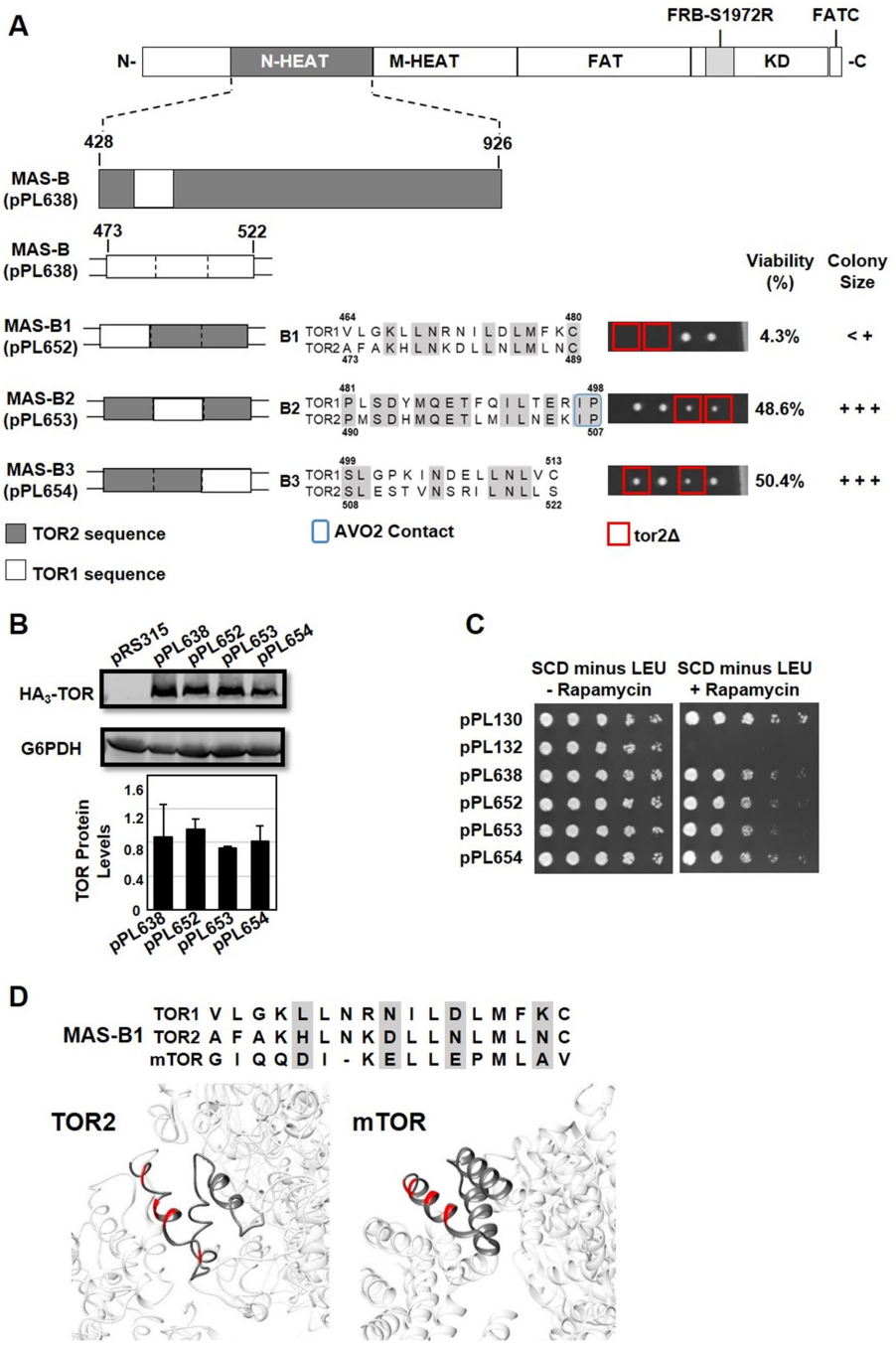

FIGURE 6: Identification of functional elements within the TOR2 MAS-B chimera. (A) MAS-B plasmid pPL638 containing the S1972R (RapR) TOR1-1 allele was modified to create the indicated TOR1-TOR2 chimeras. Each construct, B1 through B3, contains approximately 6–10 amino acids of TOR1 sequence within an otherwise TOR2 MAS domain, as depicted in the indicated sequence alignments for TOR1 and TOR2. Predicted amino acids contacts between TOR2 and AVO2 are boxed in blue in construct TOR2 MAS B-2. Plasmids were introduced into heterozygous TOR2/tor2Δ cells and analyzed by tetrad dissection as described in the legend to Figure 3A. (B) Western blot analysis of TOR1-TOR2 chimeras. TOR2/tor2Δ cells carrying the indicated plasmids were prepared and analyzed as described in the legend to Figure 2D. (C) TOR2/tor2Δ cells carrying the indicated plasmids were tested for rapamycin resistance as described in the legend to Figure 3B. (D) Sequence alignment of MAS-B1 in TOR1, TOR2, and mTOR, highlighting four nonconservative amino acid changes between TOR1 and TOR2 (shaded). Structures depict the MAS-B1 element within Cryo-EM structures of TORC2 (left) (Karuppasamy *et al.*, 2017) and mTORC2 (right) (Scaiola *et al.*, 2020). The four amino acids shaded in the alignment are highlighted in red in both structures.

TOR2 MAS domain chimera as a "sensitized" genetic background to reveal the importance of specific TOR2 sequences. Remarkably, for one segment, TOR2 MAS-B1, we were able to resolve this element to near-amino-acid resolution.

At a structural level, chimera MAS-B1 corresponds to the N-terminal helix of HEAT repeat 10, where it is positioned at the exterior of the MAS domain (Karuppasamy *et al.*, 2017) (Figure 6D). Within this segment are four nonconservative amino acid differences between TOR1 and TOR2, all predicted to lie on an external-facing edge of the helix (Figure 6D). At present, there are no predicted interactions involving these residues. Thus, one possibility is that this helix interacts with portions of AVO2 or AVO3 that have yet to be identified at the ultrastructural level or, alternatively, with a different component essential for TORC2 assembly and/or function, for example, the TTT-R2TP cochaperone complex required for proper (m)TOR folding (Takai *et al.*, 2007, 2010; Kim *et al.*, 2013). Examination of a structural model for mTORC2 reveals that this same helix within mTOR is similarly positioned at the outer surface of mTORC2 (Figure 6D) (Scaiola *et al.*, 2020). In this context, we note that, as for AVO3, a substantial portion of Rictor (approximately 35%) remains unidentified within the mTORC2 structure (Scaiola *et al.*, 2020).

The segment of TOR2 corresponding to MAS-E is predicted to be involved in interactions with both AVO3 and the other TOR2 chain within the TORC2 dimer interface (Karuppasamy *et al.*, 2017; Hill *et al.*, 2018) (Figure 7D). This arrangement of interactions is conserved in mTORC2, where corresponding sequences in mTOR are located adjacent to Rictor as well as the other mTOR chain (Scaiola *et al.*, 2020) (Figure 7D). Interestingly, for both AVO3 and Rictor, in the present structural models significant portions of both proteins are missing directly adjacent to MAS-E, suggesting that there may be additional associations with this region of TOR (Karuppasamy *et al.*, 2017; Scaiola *et al.*, 2020). Moreover, in a recent structural model for mTORC1, Raptor displays extensive interactions with sequences corresponding to MAS-E (Yang *et al.*, 2017) (Figure 7D), providing a possible rationale for why changes in this region affect both TORC1 and TORC2 activity. Alternatively, this region includes intermolecular contacts between the two mTOR proteins within the dimeric structures of mTORC1 and mTORC2 (Yang *et al.*, 2017; Scaiola *et al.*, 2020), as well as for TOR2 within TORC2 (Karuppasamy *et al.*, 2017).

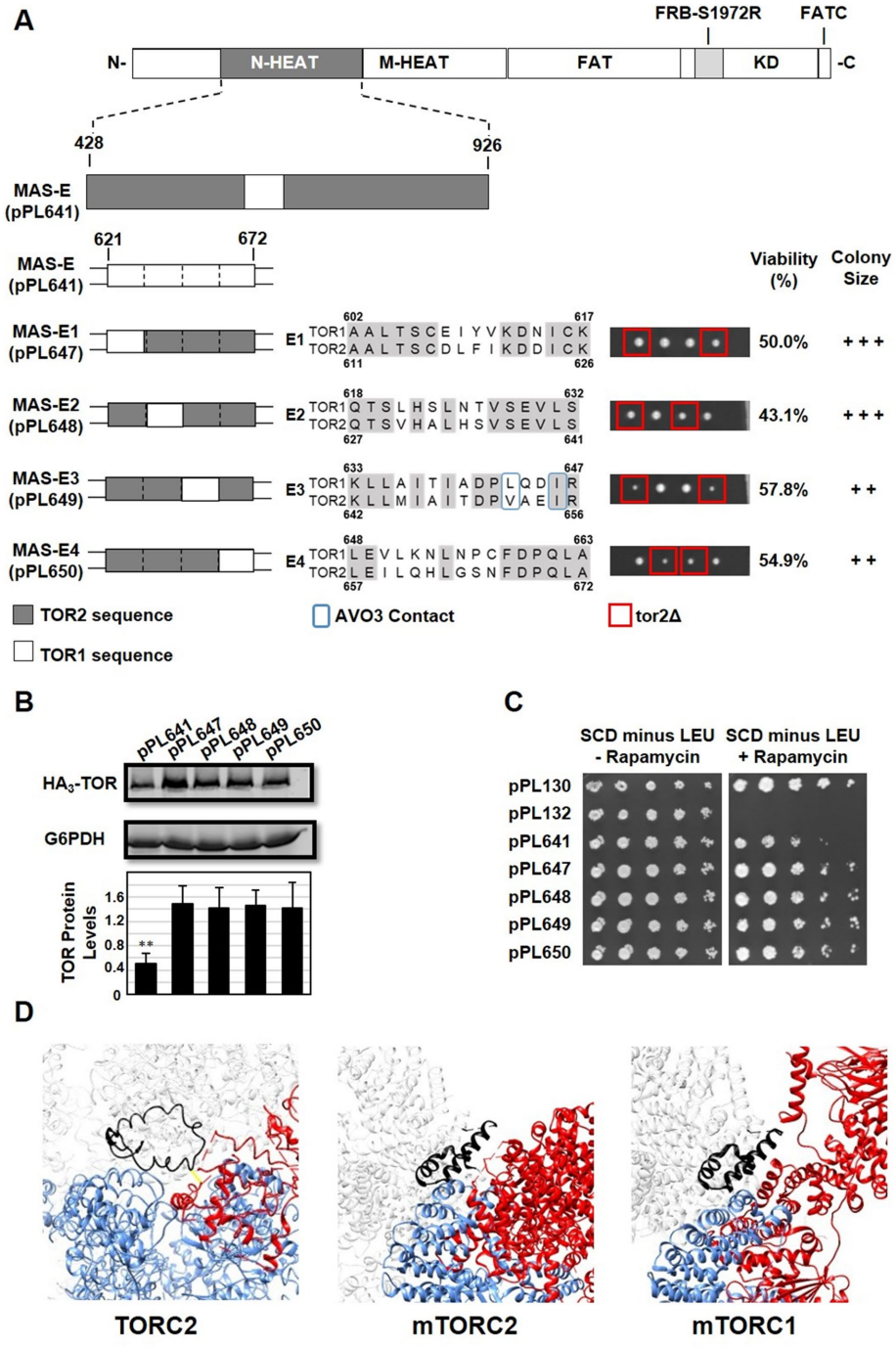

FIGURE 7: Identification of functional elements within the TOR2 MAS-E chimera. (A) MAS-E plasmid pPL641 containing the S1972R (RapR) TOR1-1 allele was modified to create the indicated TOR1-TOR2 chimeras. Each construct, E1 through E4, contains approximately 6–10 amino acids of TOR1 sequence within an otherwise TOR2 MAS domain, as depicted in the indicated sequence alignments for TOR1 and TOR2. We note that chimera E1 includes four additional TOR1-specific amino acids that are not present in MAS-E. Predicted amino acids contacts between TOR2 and AVO3 are boxed in blue in E3. Plasmids were introduced into heterozygous TOR2/tor2Δ cells and analyzed as described in the legend to Figure 3A. (B) Western blot analysis of TOR1-TOR2 chimeras. TOR2/tor2Δ cells carrying the indicated plasmids were prepared and analyzed as described in the legend to Figure 2D. (C) TOR2/tor2Δ cells carrying the indicated plasmids were tested for rapamycin resistance as described in the legend to Figure 3B. (D) Sequences corresponding to MAS-E (black) are highlighted in Cryo-EM structures for TORC2, mTORC2, and mTORC1, as indicated. Also shown are the indicated partners within each complex (red) as well as portions of TOR2 or mTOR (blue) corresponding to the other protein chain within each structure. Regions of AVO3 or Rictor absent within these structures are indicated by dashed red lines in each model. Protein chains are labeled according to nomenclature described in Karuppasamy *et al.* (2017).

We were surprised to find that several chimeras we constructed resulted in reduced steady state levels of protein, likely contributing to impaired TORC1 as well as TORC2 behavior. One possibility is that the introduction of shorter TOR1-specific sequences within these regions, for example in chimeras MAS-A (pPL637) and Minimal MAS+C (pPL636), impairs localized folding, despite these sequences functioning normally within the context of a complete TOR1 protein. A more interesting possibility is that such a chimera may juxtapose sequences specific for TORC1 versus TORC2 assembly, therefore causing localized disruptions and/or competition for crucial quaternary interactions for complex-specific partners or chaperones, resulting in destabilized chimeras susceptible to degradation. As described above, consistent with the latter possibility is the observation that chimera TORC2 MAS-E involves sequences predicted to be involved in multiple protein–protein interactions within both complexes. The MAS domain is also predicted to interact with the TTT-R2TP cochaperone complex (Takai *et al.*, 2007, 2010).

Our functional studies highlight the cooperative nature of TOR complex assembly, where distinct domains distributed throughout TOR2 are normally sufficient for the formation of TORC2. By employing TOR1-TOR2 chimeras, we have been able to identify specific regions by making them essential for TORC2 identity. These findings now point the way for more detailed analyses of their role in TORC2 assembly and function. Our approach underscores the utility of analyzing paralogues to understand the molecular basis of assembly, as well as evolution, of large protein complexes (Mirny and Gelfand, 2002; Capra *et al.*, 2012; de Juan *et al.*, 2013; Schick *et al.*, 2019; Varga *et al.*, 2021). Owing to the conservation of several important elements within mTOR, including the MAS domain, our findings point to the likely importance of these regions for both mTORC1 and mTORC2 assembly. We anticipate that applying a similar structure–function approach to mTOR will be a successful avenue for testing the importance of amino acid contacts identified in both mammalian complexes. This includes testing the importance of defined interactions between mTOR and complex-specific partners during dimer assembly as well as determining whether essential elements within the MAS domain interact with currently unidentified interacting components essential for mTOR complex assembly and signaling.

Strain	Genotype	Source
MPR1	TB50a avo3-dCT(-157aa) [HpH]	Gaubitz *et al.*, 2015
PLY 362	avo2::TRP W303a	Reinke *et al.*, 2004
PLY 1760	W303a/α tor2::HIS/TOR2 [pPL632]	This study
PLY 1761	W303a/α tor2::HIS/TOR2 [pPL655]	This study
PLY 1762	W303a/α tor2::HIS/TOR2 [pPL630]	This study
PLY 1763	W303a/α tor2::HIS/TOR2 [pPL626]	This study
PLY 1764	TOR2/tor2::HIS AVO2/avo2::TRP [pPL632]	This study
PLY 1765	TOR2/tor2::HIS AVO2/avo2::TRP [pPL626]	This study
PLY 1766	TOR2/tor2::HIS AVO2/avo2::TRP [pPL655]	This study
PLY 1767	TOR2/tor2::HIS AVO2/avo2::TRP [pPL630]	This study
PLY 1768	TOR2/tor2::HIS AVO3/avo3-dCT::HpH [pPL632]	This study
PLY 1769	TOR2/tor2::HIS AVO3/avo3-dCT::HpH [pPL626]	This study
PLY 1770	TOR2/tor2::HIS AVO3/avo3-dCT::HpH [pPL655]	This study
PLY 1771	TOR2/tor2::HIS AVO3/avo3-dCT::HpH [pPL630]	This study
PLY 1772	W303a/α tor2::HIS/TOR2 [pPL628]	This study
PLY 1773	W303a/α tor2::HIS/TOR2 [pPL629]	This study
PLY 1774	W303a/α tor2::HIS/TOR2 [pPL635]	This study
PLY 1775	W303a/α tor2::HIS/TOR2 [pPL636]	This study
PLY 1776	W303a/α tor2::HIS/TOR2 [pPL637]	This study
PLY 1777	W303a/α tor2::HIS/TOR2 [pPL638]	This study
PLY 1778	W303a/α tor2::HIS/TOR2 [pPL639]	This study
PLY 1779	W303a/α tor2::HIS/TOR2 [pPL640]	This study
PLY 1780	W303a/α tor2::HIS/TOR2 [pPL641]	This study
PLY 1781	W303a/α tor2::HIS/TOR2 [pPL642]	This study
PLY 1782	W303a/α tor2::HIS/TOR2 [pPL643]	This study
PLY 1783	W303a/α tor2::HIS/TOR2 [pPL644]	This study
PLY 1784	W303a/α tor2::HIS/TOR2 [pPL645]	This study
PLY 1785	W303a/α tor2::HIS/TOR2 [pPL646]	This study
PLY 1786	W303a/α tor2::HIS/TOR2 [pPL652]	This study
PLY 1787	W303a/α tor2::HIS/TOR2 [pPL653]	This study
PLY 1788	W303a/α tor2::HIS/TOR2 [pPL654]	This study
PLY 1789	W303a/α tor2::HIS/TOR2 [pPL647]	This study
PLY 1790	W303a/α tor2::HIS/TOR2 [pPL648]	This study
PLY 1791	W303a/α tor2::HIS/TOR2 [pPL649]	This study
PLY 1792	W303a/α tor2::HIS/TOR2 [pPL650]	This study

TABLE 1: *Saccharomyces cerevisiae* strains used in this study.

MATERIALS AND METHODS

Request a protocol through *Bio-protocol*.

Strains, media, and general methods

Strains and plasmids used in this study are listed in Tables 1 and 2, respectively. Cells were cultured in YPD (2% yeast extract, 1% peptone, and 2% dextrose) or synthetic complete dextrose (SCD) medium (0.8% yeast nitrogen base without amino acids, pH 5.5, 2% dextrose) supplemented with amino acids as described (Sherman, 1991). Rapamycin (Sigma-Aldrich, St. Louis, MO) was dissolved in dimethyl sulfoxide (DMSO) and added to SCD medium and agar plates to a final concentration of 0.2 μg/ml. Hygromycin B (Sigma-Aldrich, St. Louis, MO) was dissolved in water and added to agar plates at a final concentration of 200 μM. Yeast transformations were performed using a lithium acetate procedure (Gietz and Woods, 2002).

Construction and analysis of yeast strains for synthetic genetic interactions

Double heterozygous TOR2/tor2Δ AVO2/avo2Δ diploid strains carrying individual control or chimera plasmids were constructed by mating tor2Δ haploid strains carrying a plasmid to an avo2Δ haploid strain. Diploids were selected by growth on SCD minus leucine and tryptophan media. Following sporulation, haploid progeny were analyzed by scoring the presence or absence of markers for tor2Δ

Plasmid	Description	Chimera name	Source
pRS315	LEU2 CEN/ARS		Sikorski and Hieter, 1989
pPL130	LEU2 CEN/ARS TOR1-1		Reinke *et al.*, 2004
pPL132	LEU2 CEN/ARS TOR1		Reinke *et al.*, 2004
pPL172	pPL132, TOR2 114-1770		Hill *et al.*, 2018
pPL273	pPL130, TOR2 428-946		Hill *et al.*, 2018
pPL321	pPL130, TOR2		Hill *et al.*, 2018
pPL630	pPL172, with S1972R	N-term TOR2	This study
pPL632	pPL321, with S195R	Full-length TOR2	This study
pPL651	pPL632, TOR1 428-946, with S1975R	TOR1 MAS S1975R	This study
pPL655	pPL632, TOR1 428-946	TOR1 MAS	This study
pPL626	pPL273	TOR2 MAS	This study
pPL628	pPL626, TOR2 462-814	Minimal MAS	This study
pPL629	pPL626, TOR2 644-766	Sub-Minimal MAS	This study
pPL635	pPL626, TOR2 462-926	Minimal MAS + N	This study
pPL636	pPL626, TOR2 428-814	Minimal MAS + C	This study
pPL637	pPL626, TOR1 423-472	TOR2 MAS-A	This study
pPL638	pPL626, TOR1 473-522	TOR2 MAS-B	This study
pPL639	pPL626, TOR1 523-572	TOR2 MAS-C	This study
pPL640	pPL626, TOR1 573-622	TOR2 MAS-D	This study
pPL641	pPL626, TOR1 623-672	TOR2 MAS-E	This study
pPL642	pPL626, TOR1 673-722	TOR2 MAS-F	This study
pPL643	pPL626, TOR1 723-772	TOR2 MAS-G	This study
pPL644	pPL626, TOR1 773-823	TOR2 MAS-H	This study
pPL645	pPL626, TOR1 824-873	TOR2 MAS-I	This study
pPL646	pPL626, TOR1 874-946	TOR2 MAS-J	This study
pPL652	pPL626, TOR1 473-489	TOR2 MAS-B1	This study
pPL653	pPL626, TOR1 490-507	TOR2 MAS-B2	This study
pPL654	pPL626, TOR1 508-522	TOR2 MAS-B3	This study
pPL647	pPL626, TOR1 611-626	TOR2 MAS-E1	This study
pPL648	pPL626, TOR1 627-641	TOR2 MAS-E2	This study
pPL649	pPL626, TOR1 642-656	TOR2 MAS-E3	This study
pPL650	pPL626, TOR1 657-672	TOR2 MAS-E4	This study

TABLE 2: Plasmids used in this study.

(growth on SCD minus histidine media), avo2Δ (growth on SCD minus tryptophan), and the relevant plasmid (growth on SCD minus leucine media). Double heterozygous TOR2/tor2Δ AVO3/avo3-ΔCT diploid strains carrying individual control or chimera plasmids were constructed by mating tor2Δ haploid strains carrying a plasmid to an avo3-ΔCT haploid strain. Diploids were identified following growth in SCD minus leucine media by their ability to form spores in sporulation media. Following sporulation, haploid progeny were analyzed by scoring the presence or absence of markers for tor2Δ (growth on SCD minus histidine media), avo3-ΔCT (growth in the presence of hygromycin), and the relevant plasmid (growth on SCD minus leucine media).

Plasmid construction

Plasmids used in this study are listed in Table 2. Plasmid construction was carried out in conjunction with Genscript (Piscataway, NJ). Plasmids pPL626, pPL630, and pPL632 were constructed using previously constructed parental plasmids (Hill *et al.*, 2018) and used as templates for construction of new chimeras, as indicated in Table 2. The precise positions of switch points and specific chimeric sequences for each plasmid are listed in Supplemental Table S1, and all sequences are provided in Supplemental Table S2. Synthetic DNA sequences were subcloned into expression vectors by fragment exchange using two unique restriction sites or by modified Gibson Assembly (Casini *et al.*, 2015) (see Supplemental Table S1). Plasmids were sequenced in their entirety to confirm the accuracy of construction.

Whole cell extraction, Western blot analysis, and quantification

Cells were grown overnight to mid–logarithmic phase (A_{600} = 2.0) in SCD minus leucine media at 30°C. Protein extracts were prepared

using the NaOH cell lysis method (Dilova *et al.*, 2004). Equivalent amounts of extract were loaded onto SDS–PAGE gels and then transferred to nitrocellulose membranes. Membranes were probed with α-HA (12CA5; 1:5000 dilution; Covance) and α-G6PDH (1:100,000 dilution; Sigma-Aldrich) primary antibodies. Secondary antibodies conjugated to IRDye (1:5000 dilution; LI-COR Biosciences) were used, and blots were imaged using either an Odyssey Infrared Imaging System (LI-COR Biosciences) or an Azure Sapphire Biomolecular Imager. Images were quantified using LI-COR Image Studio Lite.

Averages of three independent biological replicates are presented with means ± SD. The *p* values were calculated using Student's *t* test: **p* between 0.05 and 0.01 and ***p* ≤ 0.01.

Molecular modeling

Molecular graphics and analyses were performed with the UCSF Chimera package (Pettersen *et al.*, 2004). The following Cryo-EM models were used for analysis: *S. cerevisiae* TORC2 (PDB accession number 6EMK) (Karuppasamy *et al.*, 2017); human mTORC2 (PDB accession number 6ZWM) (Scaiola *et al.*, 2020); and human mTORC1 (PDB accession number 6BCX) (Yang *et al.*, 2017).

ACKNOWLEDGMENTS

We thank A. Cuyegkeng for assistance with sequence alignments and modeling using UCSF Chimera, A. Cuyegkeng and M. Cadden for help with early designs of TOR2 MAS domain chimeras, and R. Loewith for the avo3-ΔCT strain. We thank E. Baldwin, K. Kaplan, and J. Nunnari for discussions and E. Baldwin, C. Fraser, M. Hall, R. Loewith, and K. Shiozaki for comments on the manuscript. This work was supported by research funds provided by the Department of Molecular and Cellular Biology and the College of Biological Sciences (to T. P.). Chimera was developed by the Resource for Biocomputing, Visualization, and Informatics at the University of California, San Francisco (supported by National Institute of General Medical Sciences P41-GM103311).

REFERENCES

Andrade MA, Bork P (1995). HEAT repeats in the Huntington's disease protein. Nat Genet 11, 115–116.

Andrade MA, Petosa C, O'Donoghue SI, Müller CW, Bork P (2001). Comparison of ARM and HEAT protein repeats. J Mol Biol 309, 1–18.

Aylett CHS, Sauer E, Imseng S, Boehringer D, Hall MN, Ban N, Maier T (2016). Architecture of human mTOR complex 1. Science 351, 48–52.

Bareti D, Berndt A, Ohashi Y, Johnson CM, Williams RL (2016). Tor forms a dimer through an N-terminal helical solenoid with a complex topology. Nat Commun 7, 11016.

Bosotti R, Isacchi A, Sonnhammer EL (2000). FAT: a novel domain in PIK-related kinases. Trends Biochem Sci 25, 225–227.

Capra EJ, Perchuk BS, Skerker JM, Laub MT (2012). Adaptive mutations that prevent crosstalk enable the expansion of paralogous signaling protein families. Cell 150, 222–232.

Casini A, Storch M, Baldwin GS, Ellis T (2015). Bricks and blueprints: methods and standards for DNA assembly. Nat Rev Mol Cell Biol 16, 568–576.

Chen X, Liu M, Tian Y, Li J, Qi Y, Zhao D, Wu Z, Huang M, Wong CCL, Wang HW, *et al.* (2018). Cryo-EM structure of human mTOR complex 2. Cell Res 28, 518–528.

de Juan D, Pazos F, Valencia A (2013). Emerging methods in protein co-evolution. Nat Rev Genet 14, 249–261.

Dilova I, Aronova S, Chen JC-Y, Powers T (2004). Tor signaling and nutrient-based signals converge on Mks1p phosphorylation to regulate expression of Rtg1.Rtg3p-dependent target genes. J Biol Chem 279, 46527–46535.

Eltschinger S, Loewith R (2016). TOR complexes and the maintenance of cellular homeostasis. Trends Cell Biol 26, 148–159.

Gaubitz C, Oliveira TM, Prouteau M, Leitner A, Karuppasamy M, Konstantinidou G, Rispal D, Eltschinger S, Robinson GC, Thore S, *et al.* (2015). Molecular basis of the rapamycin insensitivity of target of rapamycin complex 2. Mol Cell 58, 977–988.

Gietz RD, Woods RA (2002). Transformation of yeast by lithium acetate/single-stranded carrier DNA/polyethylene glycol method. Methods Enzymol 350, 87–96.

Guarente L (1993). Synthetic enhancement in gene interaction: a genetic tool come of age. Trends Genet 9, 362–366.

Hara K, Maruki Y, Long X, Yoshino K, Oshiro N, Hidayat S, Tokunaga C, Avruch J, Yonezawa K (2002). Raptor, a binding partner of target of rapamycin (TOR), mediates TOR action. Cell 110, 177–189.

Heitman J, Movva NR, Hall MN (1991). Targets for cell cycle arrest by the immunosuppressant rapamycin in yeast. Science 253, 905–909.

Helliwell SB, Wagner P, Kunz J, Deuter-Reinhard M, Henriquez R, Hall MN (1994). TOR1 and TOR2 are structurally and functionally similar but not identical phosphatidylinositol kinase homologues in yeast. Mol Biol Cell 5, 105–118.

Hill A, Niles B, Cuyegkeng A, Powers T (2018). Redesigning TOR kinase to explore the structural basis for TORC1 and TORC2 assembly. Biomolecules 8, E36.

Jacinto E, Loewith R, Schmidt A, Lin S, Rüegg MA, Hall A, Hall MN (2004). Mammalian TOR complex 2 controls the actin cytoskeleton and is rapamycin insensitive. Nat Cell Biol 6, 1122–1128.

Kaiser CA, Schekman R (1990). Distinct sets of SEC genes govern transport vesicle formation and fusion early in the secretory pathway. Cell 61, 723–733.

Karuppasamy M, Kusmider B, Oliveira TM, Gaubitz C, Prouteau M, Loewith R, Schaffitzel C (2017). Cryo-EM structure of Saccharomyces cerevisiae target of rapamycin complex 2. Nat Commun 8, 1729.

Kim D-H, Sarbassov DD, Ali SM, King JE, Latek RR, Erdjument-Bromage H, Tempst P, Sabatini DM (2002). mTOR interacts with raptor to form a nutrient-sensitive complex that signals to the cell growth machinery. Cell 110, 163–175.

Kim D-H, Sarbassov DD, Ali SM, Latek RR, Guntur KVP, Erdjument-Bromage H, Tempst P, Sabatini DM (2003). GbetaL, a positive regulator of the rapamycin-sensitive pathway required for the nutrient-sensitive interaction between raptor and mTOR. Mol Cell 11, 895–904.

Kim SG, Hoffman GR, Poulogiannis G, Buel GR, Jang YJ, Lee KW, Kim BY, Erikson RL, Cantley LC, Choo AY, Blenis J (2013). Metabolic stress controls mTORC1 lysosomal localization and dimerization by regulating the TTT-RUVBL1/2 complex. Mol Cell 49, 172–185.

Knutson BA (2010). Insights into the domain and repeat architecture of target of rapamycin. J Struct Biol 170, 354–363.

Loewith R, Jacinto E, Wullschleger S, Lorberg A, Crespo JL, Bonenfant D, Oppliger W, Jenoe P, Hall MN (2002). Two TOR complexes, only one of which is rapamycin sensitive, have distinct roles in cell growth control. Mol Cell 10, 457–468.

Magaway C, Kim E, Jacinto E (2019). Targeting mTOR and metabolism in cancer: lessons and innovations. Cells 8, E1584.

Mirny LA, Gelfand MS (2002). Using orthologous and paralogous proteins to identify specificity-determining residues in bacterial transcription factors. J Mol Biol 321, 7–20.

Mossmann D, Park S, Hall MN (2018). mTOR signalling and cellular metabolism are mutual determinants in cancer. Nat Rev Cancer 18, 744–757.

Perry J, Kleckner N (2003). The ATRs, ATMs, and TORs are giant HEAT repeat proteins. Cell 112, 151–155.

Pettersen EF, Goddard TD, Huang CC, Couch GS, Greenblatt DM, Meng EC, Ferrin TE (2004). UCSF Chimera–a visualization system for exploratory research and analysis. J Comput Chem 25, 1605–1612.

Reinke A, Anderson S, McCaffery JM, Yates J, Aronova S, Chu S, Fairclough S, Iverson C, Wedaman KP, Powers T (2004). TOR complex 1 includes a novel component, Tco89p (YPL180w), and cooperates with Ssd1p to maintain cellular integrity in Saccharomyces cerevisiae. J Biol Chem 279, 14752–14762.

Sarbassov DD, Ali SM, Kim D-H, Guertin DA, Latek RR, Erdjument-Bromage H, Tempst P, Sabatini DM (2004). Rictor, a novel binding partner of mTOR, defines a rapamycin-insensitive and raptor-independent pathway that regulates the cytoskeleton. Curr Biol 14, 1296–1302.

Saxton RA, Sabatini DM (2017). mTOR signaling in growth, metabolism, and disease. Cell 168, 960–976.

Scaiola A, Mangia F, Imseng S, Boehringer D, Berneiser K, Shimobayashi M, Stuttfeld E, Hall MN, Ban N, Maier T (2020). The 3.2-Å resolution structure of human mTORC2. Sci Adv 6, eabc1251.

Schick S, Rendeiro AF, Runggatscher K, Ringler A, Boidol B, Hinkel M, Májek P, Vulliard L, Penz T, Parapatics K, *et al.* (2019). Systematic characterization of BAF mutations provides insights into intracomplex synthetic lethalities in human cancers. Nat Genet 51, 1399–1410.

Sherman F (1991). Getting started with yeast. Methods Enzymol 194, 3–21.

Sikorski RS, Hieter P (1989). A system of shuttle vectors and yeast host strains designed for efficient manipulation of DNA in Saccharomyces cerevisiae. Genetics 122, 19–27.
Stuttfeld E, Aylett CH, Imseng S, Boehringer D, Scaiola A, Sauer E, Hall MN, Maier T, Ban N (2018). Architecture of the human mTORC2 core complex. eLife 7, e33101.
Tafur L, Kefauver J, Loewith R (2020). Structural Insights into TOR Signaling. Genes (Basel) 11, E885.
Takai H, Wang RC, Takai KK, Yang H, de Lange T (2007). Tel2 regulates the stability of PI3K-related protein kinases. Cell 131, 1248–1259.
Takai H, Xie Y, de Lange T, Pavletich NP (2010). Tel2 structure and function in the Hsp90-dependent maturation of mTOR and ATR complexes. Genes Dev 24, 2019–2030.
Varga J, Kube M, Luck K, Schick S (2021). The BAF chromatin remodeling complexes: structure, function, and synthetic lethalities. Biochem Soc Trans 49, 1489–1503.
Wedaman KP, Reinke A, Anderson S, Yates J, McCaffery JM, Powers T (2003). Tor kinases are in distinct membrane-associated protein complexes in Saccharomyces cerevisiae. Mol Biol Cell 14, 1204–1220.
Wullschleger S, Loewith R, Hall MN (2006). TOR signaling in growth and metabolism. Cell 124, 471–484.
Wullschleger S, Loewith R, Oppliger W, Hall MN (2005). Molecular organization of target of rapamycin complex 2. J Biol Chem 280, 30697–30704.
Yang H, Wang J, Liu M, Chen X, Huang M, Tan D, Dong MQ, Wong CC, Wang J, Xu Y, Wang HW, *et al*. (2016). 4.4 Å resolution cryo-EM structure of human mTOR complex 1. Protein Cell 7, 878–887.
Yang H, Jiang X, Li B, Yang HJ, Miller M, Yang A, Dhar A, Pavletich NP (2017). Mechanisms of mTORC1 activation by RHEB and inhibition by PRAS40. Nature 552, 368–373.
Yang H, Rudge DG, Koos JD, Vaidialingam B, Yang HJ, Pavletich NP (2013). mTOR kinase structure, mechanism and regulation. Nature 497, 217–223.